NASA TN D-507

TECHNICAL NOTE

D-507

RADIO TRANSMISSION THROUGH THE PLASMA SHEATH

AROUND A LIFTING REENTRY VEHICLE

By Macon C. Ellis, Jr., and Paul W. Huber

Langley Research Center
Langley Field, Va.

NATIONAL AERONAUTICS AND SPACE ADMINISTRATION

WASHINGTON

January 1961

NATIONAL AERONAUTICS AND SPACE ADMINISTRATION

TECHNICAL NOTE D-507

RADIO TRANSMISSION THROUGH THE PLASMA SHEATH AROUND A LIFTING REENTRY VEHICLE

By Macon C. Ellis, Jr., and Paul W. Huber

SUMMARY

A review is made of the general concepts of radio-signal attenuation related to the plasma sheath around a hypersonic reentry vehicle. Plasma-attenuation experiments are described in which telemetry and microwave signals are transmitted through a plasma closely simulating that on a lifting hypersonic reentry vehicle.

Computations are made of the plasma conditions about simple-shaped bodies for the case of real-air, hypersonic, viscous flow. The peak plasma frequency occurs in the shock layer just outside the boundary layer for all cases except for sharp-nose bodies at low angle of attack. The magnitude of the peak plasma frequency at a given aft location is strongly dependent upon the bluntness of the body, and is dependent to a lesser extent on the location along the body. The variation of peak plasma frequency in the shock layer at an aft location for various lifting reentry trajectories is presented to show effects of lift coefficient, wing loading, altitude, and velocity. Plasma collision frequency is also shown to be much less than the plasma frequency during the critical (or maximum plasma frequency) part of the flight. It is concluded that signal frequencies of the order of 10 kmc are required to avoid sudden loss of communications during the critical part of a lifting reentry hypersonic vehicle flight.

A brief discussion is given of the areas of research needed in order to understand the plasma-attenuation problem better as well as to indicate the methods of alleviating this problem.

INTRODUCTION

The problem of transmitting radio-frequency signals to and from a high-altitude hypersonic vehicle can be divided into three parts if those

components of the system within the vehicle and on the ground are excluded from consideration. These parts are:

1. Propagation of electromagnetic waves through the atmosphere.

2. Propagation of electromagnetic waves through the ionized gas or plasma surrounding the vehicle.

3. Radiation problems connected with the antenna coupling with the conducting gas.

The present paper is confined to part 2, the plasma-sheath problem, as simply shown in figure 1. The plasma sheath is depicted in the figure as the shaded region enclosed by the shock wave about the vehicle, and a transmitting antenna is indicated at a rearward station on the lower surface. The plasma-sheath problem can be further divided into two parts, namely, the determination of plasma conditions about the vehicle for given flight conditions and the determination of the effects of this plasma on the transmitted signal. The ability to analyze the second of these - the effect of the plasma on the signal - is in much better shape than the ability to specify the given plasma conditions, so that the prime problems at the present time appear to be aerodynamic and thermodynamic ones. However, first a review is given of the simplest theoretical approach in studying the effects of the plasma on the transmitted signal. The electromagnetic-radiation theory utilized is for plane-wave, linearly polarized, monochromatic radiation, and this radiation is assumed to interact with a homogeneous plasma in thermodynamic equilibrium. The primary parameters in this problem are shown in the lower part of the figure, where, first, the signal frequency is obviously the independent variable. Even though the plasma has no net charge outside some minimum distance (the Debye length) within the plasma, it contains free electrons and there exists a natural oscillation of an average free electron at the so-called plasma frequency. The concentration of these free electrons in the gas determines the plasma frequency f_p; it is proportional to the square root of the electron density. The electron-collision frequency f_c is roughly the average number of times an average electron collides elastically with a heavier particle (ion or neutral). It is emphasized that these quantities are obtained from the state properties of the gas only - for example, temperature and density - and once these properties are known for the flow conditions about the given vehicle, then f_p and f_c are known. The last parameter shown in the lower part of figure 1 is simply the plasma thickness which the wave has to negotiate.

Various aspects of the factors in the plasma-sheath problem have been discussed in some detail in references 1 to 9. After first reviewing

the application of the simple plane-wave theory to transmission through a plasma, the present paper gives results from experiments designed to check this theory. Finally, results of calculations of the plasma conditions about lifting reentry vehicles are presented and estimates made of the transmission frequency required.

SYMBOLS

A	signal attenuation measured in decibels
C_L	lift coefficient, $\frac{L}{\frac{1}{2}\rho V^2 S}$
f	transmitted signal frequency, kmc
f_c	plasma electron-collision frequency, $\nu/2\pi$, kmc
f_p	plasma resonant frequency, kmc
$f_{p,MAX}$	maximum plasma resonant frequency attained during trajectory, kmc
h	altitude, ft
L	lift, lb
M	Mach number
p	absolute pressure, atm
r/R	radial distance from center line of body in terms of body radius
S	wing surface area, sq ft
T	temperature, ^{o}K
t	plasma thickness, ft
V	velocity, ft/sec
W/S	wing loading, lb/sq ft
x,y	distances along X- and Y-axes, respectively, ft

x/R	longitudinal distance from nose of body in terms of body radius
α	angle of attack, deg
λ	wavelength, cm
ν	electron-collision frequency (collisions per second), kmc
ρ	mass density, slugs/cu ft
ψ_1	streamline identification (fig. 7)

ATTENUATION CONCEPTS RELATED TO HYPERSONIC REENTRY

Plane-Wave Theory

The solution of the plane-wave attenuation equations for the transmitted portion of the incident signal is shown in figure 2 in the form of attenuation per unit plasma thickness, normalized to the plasma frequency, as a function of signal frequency and collision frequency, nondimensionalized to the plasma frequency. For the collision-frequency parameter f_c/f_p, low values may be regarded as corresponding to high altitudes and high values, to low altitudes. The curve for $f_c/f_p = 0.01$ (high altitude) shows a steep or sudden decrease in attenuation as the value of $f/f_p = 1$ is exceeded so that for values of f/f_p just greater than 1, attenuation is negligible. For intermediate values of f_c/f_p, no such sharp decrease in attenuation is indicated and attenuation values are moderately high over a large range of f/f_p which includes values on both sides of $f/f_p = 1$. For high values of f_c/f_p (low altitudes), low attenuation is seen for a still broader range of f/f_p. Lastly, it is to be noted that not only does attenuation decrease at high values of f/f_p, but also it decreases toward low values of f/f_p; however, in this very low frequency range, atmospheric noise is a problem and large antennas may be required.

Attenuation Trajectories

Figure 3 shows attenuation trajectories of a possible lifting vehicle reentering from satellite velocity for one flight path and two fixed-frequency transmitters. In understanding this figure, one simple

fact needs to be known first - the fact that the plasma frequency at a point on a vehicle during reentry rises from low values at very high altitudes to a maximum at intermediate altitudes and then decreases again to low values during the latter part of the reentry. The change of attenuation during reentry is seen by following the arrows. The trajectory conditions are as follows: W/S = 27 lb/sq ft, C_L = 0.12, and $f_{p,MAX}$ = 8 kmc. Estimates of plasma conditions throughout the trajectory have been made for an aft location where the antenna is assumed to be located. For the 3-kmc case, the signal frequency greatly exceeds the plasma frequency for the initial part of the reentry, becomes equal (at $f/f_p = 1$) at some point as the gas temperature around the vehicle increases and f_p increases, and becomes less than the maximum value of f_p of 8 kmc at some lower altitude of the reentry. For this case, attenuation is very high near the loop in the curve. As the reentry vehicle proceeds to still lower altitudes and the plasma sheath becomes cooler, f is still less than f_p, but collision frequencies, that is, f_c/f_p, increase at the lower altitudes; thus, the signal strength is regained more slowly than it was cut off. For the 10-kmc case, signal frequency is always higher than the plasma frequency and thus low attenuations are seen throughout the reentry. This latter case corresponds to the lower, right portion of figure 2, where other generalized attenuation curves for intermediate values of f_c/f_p would also lie.

PLASMA-ATTENUATION EXPERIMENTS

Plasma Production and Diagnosis

The question at this point is the applicability of the plane-wave theory to the plasma-sheath problem. For many years, physicists have used microwave techniques in plasma diagnostics; however, most of their cases have been highly specialized and the phenomena were fairly well known from other observations (refs. 10 to 12). Also, much effort has been spent in diagnosing plasma conditions in rocket-exhaust flames. In most of these cases, however, nonequilibrium effects leading to so-called "chemi-ionization" have been present to confuse the picture. (See ref. 13 which also contains an excellent review and bibliography.) In the Langley Gas Dynamics Branch, a fairly large flame has been developed in which nonequilibrium ionization effects are absent. This flame has been used as the plasma source for studying the electromagnetic-wave—plasma interaction problem in a joint program involving also the Langley Instrument Research Division. (See ref. 14.) In this system, cyanogen and oxygen are burned to produce the primary combustion products of carbon monoxide and nitrogen at a temperature over 4,000° K after

cooling losses. In this flame, a significant ionization of these and small quantities of other products occurs, and this flame plasma closely simulates certain lifting reentry plasma conditions. Apparatus and methods have also been established which allow introduction and mixing into the flame of vaporized potassium, yielding ionization levels even higher than those for gas conditions at the nose of an ICBM. Results to be discussed here are only for the flame without potassium seeding. Earlier work on the combustion of cyanogen and oxygen and the thermodynamic properties of cyanogen are given in references 15 to 25.

Attenuation Results With Cyanogen Flame

Figure 4 shows, at the right, cross sections of the burner chamber and nozzle of the apparatus. (The nozzle is 7.5 cm in diameter.) The theoretical curve is from the generalized attenuation calculations in figure 2, where the value of f_c/f_p, for this case, is 1.5 and was determined from independent flame temperature measurements. The experiments cover a range of frequencies from 0.2 to 20 kmc. With regard to the 20-kmc result (λ = 1.5 cm) where the microwave beam is transverse to the flame as shown in the bottom sketch, the space resolution should be good since for this case the receiving horn "views" a small section of the flame. The check of the theory is good, within the experimental scatter. For the 8-kmc case (λ = 3.75 cm), however, the space resolution with this transverse beam is not as good and edge effects would be expected; these results consequently show poorer agreement with theory. For the 9.4-kmc case (λ = 3.2 cm), but for a different test configuration as shown by the middle sketch, the agreement is again satisfactory as might be expected since, for this case, the waveguide radiator transmits through a nearly flat plasma sheet and edge effects should be minimized. For the 0.2-kmc case (λ = 137 cm), it might be expected that near-field effects would invalidate the plane-wave theory; however, a surprisingly good check is noted. For this last case, the radiator is an axisymmetric dipole immersed in the flame as shown by the top sketch.

The flame has been used for a direct check of the theory for the results shown in figure 4; however, its principal use is to aid in the study of as many other related problems as possible - for example, antenna details, power loading, radiation patterns, harmonics, polarization, phase shift, and so forth. The result at 9.4 kmc is, as a matter of fact, for a peak power of about 40 kilowatts; thus, it is indicated that power loading up to this value has not affected the plasma which is at a possible flight condition. This last point should be taken as a preliminary result since calculations in progress by other staff members in the Gas Dynamics Branch are indicating possibilities of significant changes from the assumed equilibrium plasma model for short, high-power pulses.

PLASMA CONDITIONS FOR LIFTING REENTRY

Although the general applicability of plane-wave theory has certainly not been proved with finality, it can be applied to flight cases with some confidence. The relative magnitudes of plasma frequencies for several reentry flight cases are shown in figure 5. The plasma frequency is shown as a function of velocity for actual trajectories representing two flow extremes. For the illustrative ICBM case, plasma conditions have been calculated as those behind a normal shock. Normal-shock flow is certainly not typical for actual transmission conditions but this case is presented to show a most extreme case. The maximum value of f_p is seen to be so high that no transmitter is available to just exceed this frequency and thus to avoid intolerable attenuation. The plasma-frequency variation for a glide trajectory for normal-shock plasma conditions falls in a different range of f_p values from that for the ICBM but is pessimistically high. Also, if the overly optimistic assumption of flat-plate oblique-shock conditions for the glider is made, a too low bracketing number will be gotten. Thus, it can be seen that if the transmission frequency is to exceed the plasma frequency, signal frequencies somewhere between 1.0 and 60 kmc will be required. The problem is to determine where in this broad frequency range a realistic case will lie.

Oblique-Shock Plasma Conditions

For the actual vehicle, it is obviously not possible to calculate accurately the flow field pertinent to the transmission problem. The approach in the present paper is to consider the boundary-layer effects first, with the initial assumption of oblique-shock conditions at some typical station on the lower surface of the lifting hypersonic vehicle as those flow conditions just outside the boundary layer. There appears some justification of this simplified flow model, since the surface pressures for this case (at sufficiently high angles of attack) are about the same as those obtained by using modified Newtonian theory. With some prejudgment of critical flight conditions, a Mach number of 20 and an altitude of 200,000 feet is selected for the estimate of plasma conditions as shown in figure 6. Real-gas conditions for thermodynamic equilibrium have been used in calculating the flow; then, this flow was used as external conditions for the boundary-layer calculation. Real-gas oblique-shock conditions were calculated with the use of references 26 to 31. The laminar-boundary-layer calculations are similar, compressible solutions made on the IBM 704 electronic data processing machine by a program developed by Ivan E. Beckwith and Nathaniel B. Cohen of the Langley Research Center for a real gas using the correlation formula for density and transport properties of equilibrium dissociated

air presented in reference 32. All the calculations made for the present study were for zero pressure gradient. A wall temperature of 2,000° R was used in the calculation; however, the peak plasma conditions were found to be insensitive to variations in wall temperature. The results, shown in figure 6 in the form of plasma frequencies as a function of y and α, indicate that peak plasma frequencies at low values of α are the result of heating due to large dissipation at the low external stream enthalpies but that at the highest values of α peak plasma frequencies occur in the outer shock layer.

Nose Bluntness Effects

In the simplified flow model just presented, constant conditions in the shock layer have been assumed, and no effects of thickness or bluntness were taken into account. The effects of bluntness are extremely important and must be recognized since the nose must be blunt in order to keep aerodynamic heating rates to acceptable values. Figure 7 shows a result from reference 33 of flow-field calculations for a spherical nose-cylinder body made by using a characteristics solution with real air in thermodynamic equilibrium. The most important basic fact to note is that, as shown by the streamlines in the sketch at the top of the figure, a large fraction of the flow in the shock layer has been processed by the normal or nearly normal shock at the nose. This means that a thick region of high-entropy air (highest at the body) envelopes the body and that this must be properly taken into account in calculating the flow. In the lower part of figure 7, the pressures p and temperatures T at two downstream stations are shown in the small plots merely to indicate the qualitative variations. To be noted is the large temperature increase in moving from the shock to the surface of the body. For a two-dimensional body with the same cross section, it is obvious that the shock is displaced outward and that the absolute thickness of the high-entropy layer will be even thicker. Thus, for a thick-wing three-dimensional flight configuration, the entropy layer will be proportionately thicker than shown here. It should be mentioned that two-dimensional perfect-gas characteristics solutions made for bodies with "sonic-wedge" noses also exhibit the increase in temperature near the surface, but include no real-gas effects. In figure 8, one of these two-dimensional solutions has been used and certain assumptions have been made to estimate a real-gas case. In the case shown in the figure, all the real-gas characteristics solutions available have been used (including unpublished results obtained from Avco Corp. and General Electric Co.) and, together with estimates from the perfect-gas solutions, estimates made of the entropy distribution between the shock and surface, where the surface value is that behind a normal shock. The pressures have been assumed to be unaffected by the other errors. The final result to be seen from figure 8 is that the peak plasma frequency is about 10 kmc. The viscous boundary

layer is only about 1/3 foot in thickness. Figure 9 shows also the distribution of the collision frequency in the shock layer. It is seen that at the peak value of f_p, f_c/f_p is a small value. This fact implies sharp signal cutoff when the signal frequency drops below the plasma frequency.

Estimates of Plasma Conditions for Lifting Reentry Trajectories

Possible trajectories have been calculated and corresponding peak plasma frequencies estimated for a wing loading of 50 lb/sq ft and for the C_L values shown in figures 10 and 11. For these estimates, oblique-shock pressures and normal-shock entropies have been used. It is noted first that the somewhat more elegant estimate of figures 8 and 9 for 20,000 ft/sec ($M \approx 20$) checks the f_p values shown in figure 11 for $C_L = 0.12$, that is, about 10 kmc. The ticks on the f_p curves indicate that at velocities higher than these, the value of the collision-frequency parameter f_c/f_p is less than 0.1; thus, the plasma frequency can be regarded as the value of transmitted-signal frequency for sharp cutoff. The primary result to be noted is that a maximum exists and that its value increases with increasing lift coefficient for a given wing loading. The radar bands at the right show that even X-band radar (3.2 cm) will be cut off for a range of velocities around the maximum for the higher value of C_L. Figures 12 and 13 show similar results for a lower wing loading of 27 lb/sq ft. In figure 13, the maximum values are lower than those in figure 11, and for these cases it is seen that X-band frequencies will be transmitted since they are higher. In all the cases calculated, peak plasma frequencies were external to the boundary layer.

At this point, an estimate can be made of the signal frequency required for a critical flight condition. Figure 14 shows signal attenuation in decibels as a function of signal frequency. In this figure are shown curves for the combined attenuation effects of water vapor and oxygen which are integrated values through the atmosphere for the critical flight condition estimated by using reference 34. For the constant plasma frequency of 10 kmc, two plasma thicknesses are shown to allow for the uncertainty in estimation of the thickness of this peak plasma frequency region. In both cases, the signal frequency required to avoid both plasma attenuation and water-vapor absorption is seen to be between 11 and 13 kmc.

CONCLUDING REMARKS

Engineering estimates have been made for certain requirements for radio-frequency transmission through the plasma sheath surrounding a lifting reentry hypersonic vehicle. First, it appears that the frequencies required to transmit downward and forward from the vehicle are of the order of 10 kmc. For such transmission, sharp leading edges would alleviate the magnitude of frequency required but their use is obviously precluded from heating considerations. Lastly, it appears that rearward locations of the antenna are most favorable.

In regard to more refined estimates of the transmission problem, it appears that increasing knowledge of gas characteristics, both equilibrium and nonequilibrium, makes feasible the effort to improve electromagnetic-wave-plasma interaction calculations utilizing more complete theory than the plane-wave model; however, inability to specify the plasma conditions accurately remains a deterrent. Although no serious doubts exist as to ability to select a frequency that will penetrate a given plasma, many detail problems still need study for the complete system - that is, high-power microwave-plasma interaction effects (where nonequilibrium plasma effects may be relieving factors), antenna breakdown, antenna patterns, acquisition, and so forth.

It must not be overlooked that other possibilities exist which may alleviate or even eliminate parts of the transmission problem. Placement of the antenna on the upper surface or rear of the configuration deserves serious consideration. For example, it appears possible that an antenna for a low-frequency system could be placed on the top surface near the rear of the vehicle so that it "looked" at a receiver obliquely through the wake. At some aft location in the wake, the plasma conditions would allow for transmission of the signal frequency through the wake. Much work is being done at the present time to estimate wake plasma conditions in regard to the radar cross section of wakes of high-speed objects. (See Avco-Everett Research Report 82.)

Consideration of the fact that the downward or forward direction of transmission of electromagnetic radiation may be a requirement for lifting vehicles, continuing investigations appear necessary for better solutions to the problem (other than the use of extreme frequencies). Such investigations should include (1) study of methods of quenching ionization or increasing electron collisions, (2) study of use of magnetic fields across the plasma, (3) study of possible systems utilizing the plasma as the radiator, and (4) study of use of ablating or consumable antennas.

Langley Research Center,
National Aeronautics and Space Administration,
Langley Field, Va., April 12, 1960.

REFERENCES

1. Goldberg, P. A.: Electrical Properties of Hypersonic Shock Waves and Their Effect on Aircraft Radio and Radar. Doc. No. D2-1997, Boeing Airplane Co., June 10, 1957.

2. Homic, Stephen G., and Phillips, Richard L.: Communicating With the Hypersonic Vehicle. Astronautics, vol. 4, no. 3, Mar. 1959, pp. 36-37, 92-98.

3. Sisco, W., and Fiskin, J. M.: Shock Ionization Changes EM Propagation Characteristics. Space/Aero., vol. 31, no. 3, Mar. 1959, pp. 66-70.

4. White, J. R.: Communication During Re-Entry Blackout. [Preprint] 963-59, presented at the Am. Rocket Soc. 14th Annual Meeting (Washington, D. C.), Nov. 1959.

5. Bleviss, Z. O.: Transmission of Electromagnetic Waves Through Ionized Air Surrounding Hypersonic Aircraft. Rep. No. SM-22965, Douglas Aircraft Co., Inc., Oct. 1957.

6. MacMurraugh, Kilburn: Attenuation of Radio Waves as a Result of Boundary Layer Heating in Missiles Traveling at Supersonic Speeds. NAVORD Rep. 5816, Rev. 1 (NOTS TP 2163), U.S. Naval Ord. Test Station (China Lake, Calif.), Jan. 15, 1959.

7. Tischer, F. J.: Wave Propagation Through Ionized Gas in Space Communications. Rep. No. 59-34, Inst. Aero. Sci., Jan. 1959.

8. Lin, S. C.: A Rough Estimate of the Attenuation of Telemetering Signals Through the Ionized Gas Envelope Around a Typical Re-Entry Missile. Res. Rep. 74 (Contract No. AF04(645)-18), Avco-Everett Res. Lab., Feb. 1956.

9. Feldman, Saul: Trails of Axi-Symmetric Hypersonic Blunt Bodies Flying Through the Atmosphere. Res. Rep. 82 (Contract No. DA-19-020-ORD-4765), Avco-Everett Res. Lab., Dec. 1959.

10. Rudlin, Leonard: Preliminary Results of a Determination of Temperatures of Flames by Means of K-Band Microwave Attenuation. NACA RM E51G20, 1951.

11. Schultz, D. L.: Research at the National Physical Laboratory on the Ionization Properties of Gases at High Temperatures. NPL/Aero/378, British A.R.C., June 1957.

12. Shuler, Kurt E., and Weber, Joseph: A Microwave Investigation of the Ionization of Hydrogen-Oxygen and Acetylene-Oxygen Flames. Jour. Chem. Phys., vol. 22, no. 3, Mar. 1954, pp. 491-502.

13. Balwanz, W. W.: Ionization in Rocket Exhausts - A Survey. NRL Rep. 5193, U.S. Naval Res. Lab., Aug. 25, 1958.

14. Huber, Paul W., and Gooderum, Paul B. (With Appendix A by Theo E. Sims and Duncan E. McIver, Jr., and Appendix B by Joseph Burlock and William L. Grantham): Experiments With Plasmas Produced by Potassium-Seeded Cyanogen Oxygen Flames for Study of Radio Transmission at Simulated Reentry Vehicle Plasma Conditions. NASA TN D-627, 1960.

15. Conway, J. B., Wilson, R. H., Jr., and Grosse, A. V.: The Temperature of the Cyanogen-Oxygen Flame. Jour. American Chem. Soc. (Communications to Ed.), vol. 75, no. 2, Jan. 20, 1953, p. 499.

16. Conway, J. B., Smith, W. F. R., Liddell, W. J., and Grosse, A. V.: The Production of a Flame Temperature of 5000° K. Jour. American Chem. Soc. (Communications to Ed.), vol. 77, no. 7, Apr. 5, 1955, pp. 2026-2027.

17. Conway, J. B., and Grosse, A. V.: The Cyanogen-Oxygen Flame Under Pressure. Jour. American Chem. Soc., vol. 80, no. 12, June 20, 1958, pp. 2972-2976.

18. Doyle, William L.: High Temperature Propellant Systems Using the Liquids: Fluorine, Oxygen, Cyanogen and Hydrogen Cyanide. [Preprint] 736-58, presented at the Am. Rocket Soc. 13th Annual Meeting (New York), Nov. 1958.

19. Hord, Richard A., and Pennington, J. Byron: Temperature and Composition of a Plasma Obtained by Seeding a Cyanogen-Oxygen Flame With Cesium. NASA TN D-380, 1960.

20. Stevenson, D. P.: The Thermodynamic Functions of Cyanogen and the Cyanogen Halides. Jour. Chem. Phys., vol. 7, no. 3, Mar. 1939, pp. 171-174.

21. Thompson, H. W.: The Free Energy of Methyl Cyanide, and Equilibrium Constants of Some Related Reactions. Trans. Faraday Soc., vol. 37, no. 7, July 1941, pp. 344-352.

22. Thomas, N., Gaydon, A. G., and Brewer, L.: Cyanogen Flames and the Dissociation Energy of N_2. Jour. Chem. Phys., vol. 20, no. 3, Mar. 1952, pp. 369-374.

23. Vallee, Bart L., and Bartholomay, Anthony F.: Cyanogen-Oxygen Flame. Analytical Chem., vol. 28, no. 11, Nov. 1956, pp. 1753-1755.

24. Welcher, Richard P., Berets, Donald J., and Sentz, Lemuel E.: Stability of Cyanogen. Ind. and Eng. Chem., vol. 49, no. 10, Oct. 1957, pp. 1755-1758.

25. Grosse, A. V., and Stokes, C. S.: Study of Ultra High Temperatures. AFOSR-TR-59-168, Res. Inst. of Temple Univ., Apr. 30, 1959.

26. Huber, Paul W.: Tables and Graphs of Normal-Shock Parameters at Hypersonic Mach Numbers and Selected Altitudes. NACA TN 4352, 1958.

27. Feldman, Saul: Hypersonic Gas Dynamic Charts for Equilibrium Air. AVCO Res. Lab., Jan. 1957.

28. Logan, J. G., Jr., and Treanor, C. E.: Tables of Thermodynamic Properties of Air From 3000° K to 10,000° K at Intervals of 100° K. Rep. No. BE-1007-A-3, Cornell Aero. Lab., Inc., Jan. 1957.

29. Fiskin, J. M., Roberts, C. A., and Sisco, W. B.: Equilibrium Composition of Air Below 3,000 Degrees Kelvin Including Electron Densities. Eng. Rep. No. LB-30078, Douglas Aircraft Co., Inc., Apr. 6, 1959.

30. Anon.: Normal and Oblique Shock Characteristics at Hypersonic Speeds. Eng. Rep. No. LB-25599 (ARDC TR-57-184, AD 116202), Douglas Aircraft Co., Inc., Dec. 31, 1957.

31. Trimpi, Robert L., and Jones, Robert A.: A Method of Solution With Tabulated Results for the Attached Oblique Shock-Wave System for Surfaces at Various Angles of Attack, Sweep, and Dihedral in an Equilibrium Real Gas Including the Atmosphere. NASA TR R-63, 1960.

32. Cohen, Nathaniel B.: Correlation Formulas and Tables of Density and Some Transport Properties of Equilibrium Dissociating Air for Use in Solutions of the Boundary-Layer Equations. NASA TN D-194, 1960.

33. Feldman, Saul: A Numerical Comparison Between Exact and Approximate Theories of Hypersonic Inviscid Flow Past Slender Blunt-Nosed Bodies. Res. Rep. 71, Avco-Everett Res. Lab., June 1959.

34. Wilcox, Charles H.: Effects of Atmospheric Attenuation on Reconnaissance Antenna Design. Sci. Rep. No. 1 (AFCRC-TN-57-197, Contract AF19(604)-1708) Res. Labs., Hughes Aircraft Co., Feb. 20, 1957. (Available from ASTIA as Doc. No. AD 117038.)

RADIO TRANSMISSION FROM HYPERSONIC VEHICLE

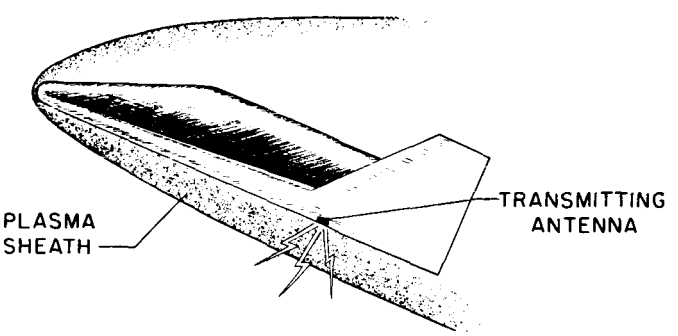

PLASMA TRANSMISSIBILITY PARAMETERS

- f SIGNAL FREQUENCY, KMC
- f_p PLASMA FREQUENCY, KMC
- f_c PLASMA ELECTRON-COLLISION FREQUENCY, KMC
- t PLASMA THICKNESS, FT

Figure 1

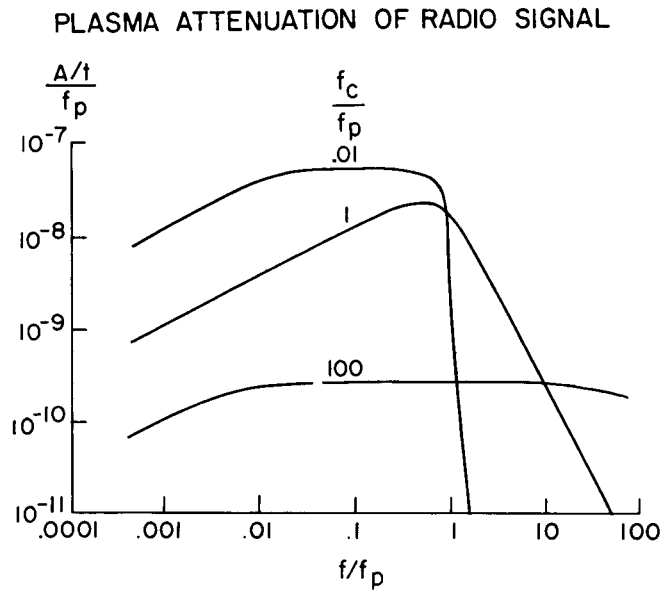

Figure 2

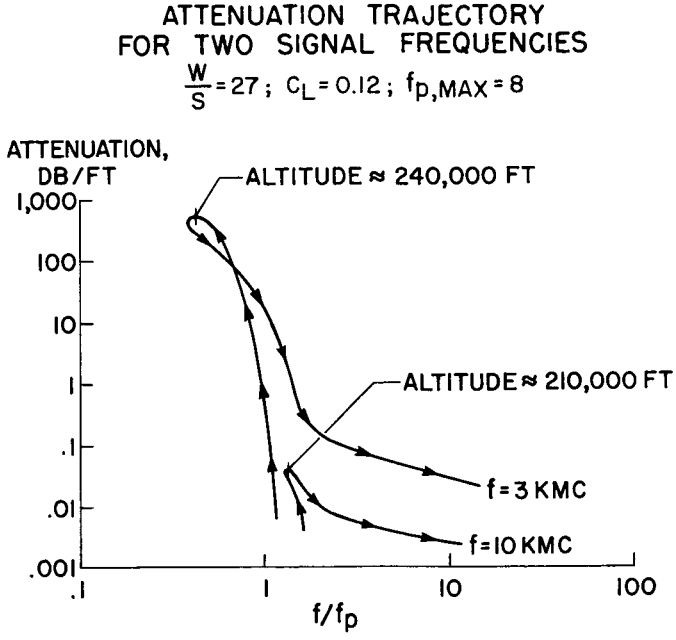

Figure 3

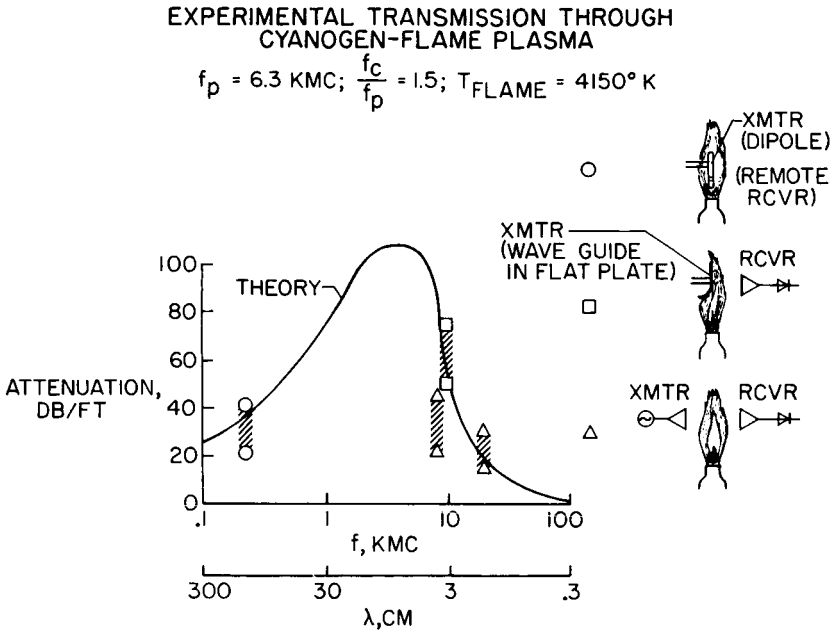

Figure 4

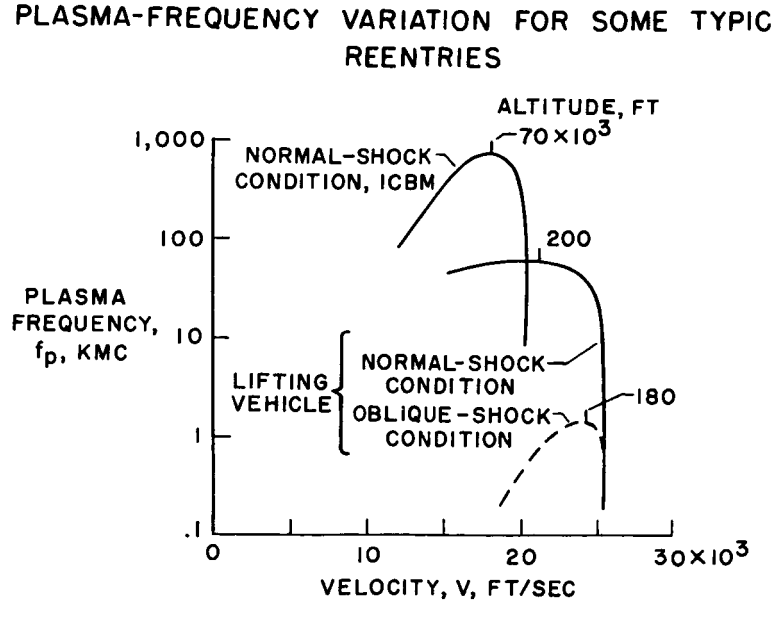

Figure 5

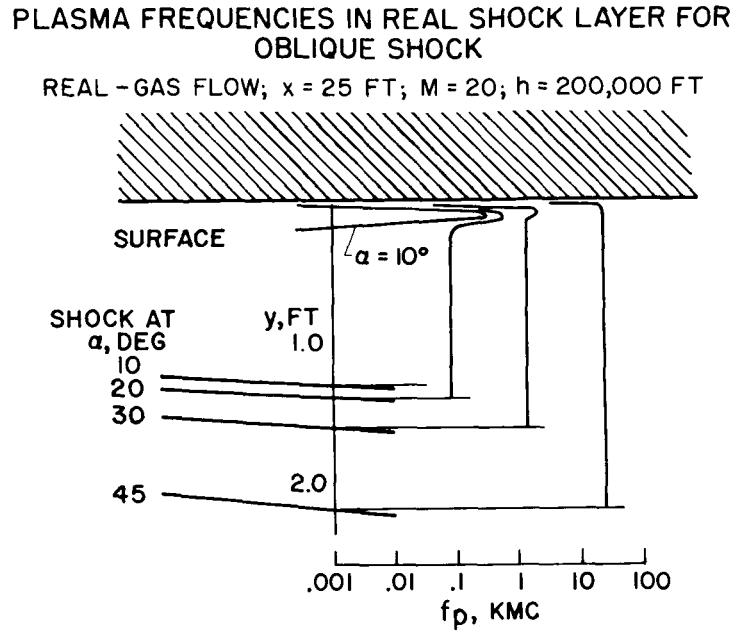

Figure 6

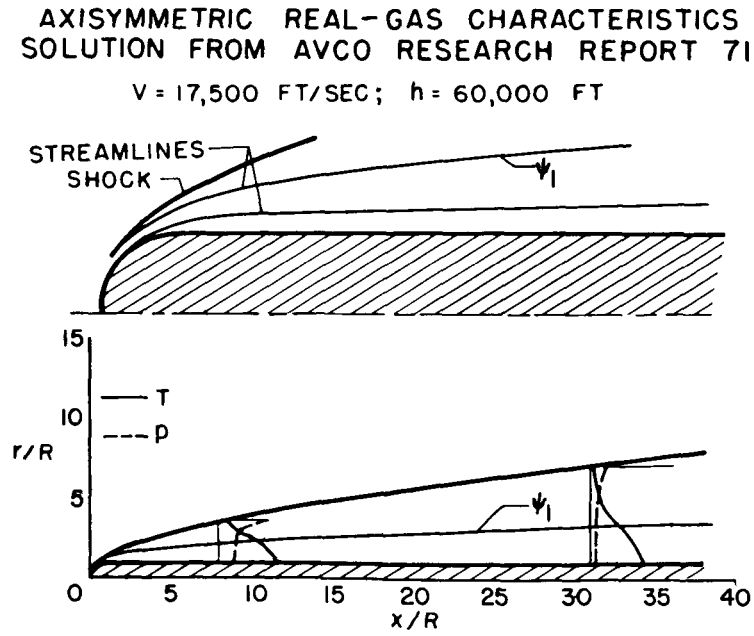

Figure 7

SHOCK-LAYER GAS CONDITIONS FOR LOWER SURFACE OF TWO-DIMENSIONAL SLAB

M = 20; α = 13°; h = 200,000 FT; x = 25 FT

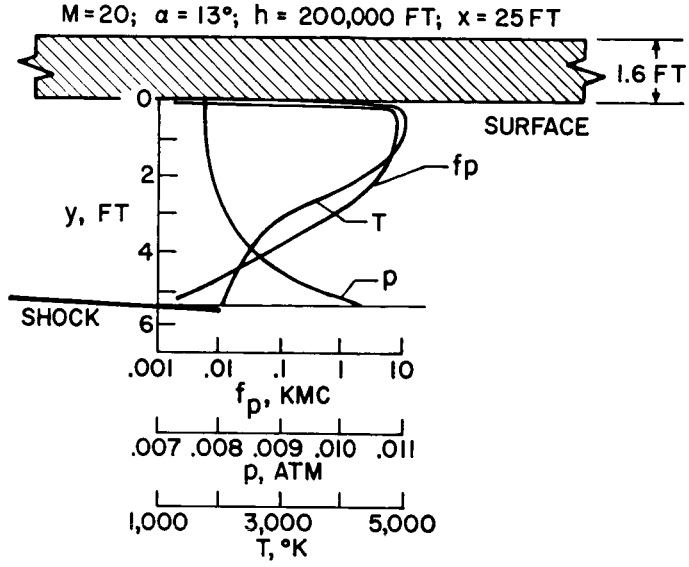

Figure 8

SHOCK-LAYER PLASMA CONDITIONS FOR LOWER SURFACE OF TWO-DIMENSIONAL SLAB

M = 20; α = 13°; h = 200,000 FT; x = 25 FT

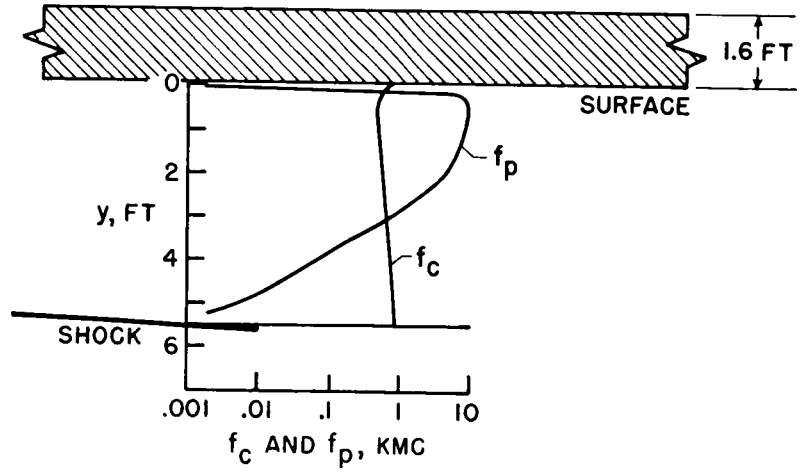

Figure 9

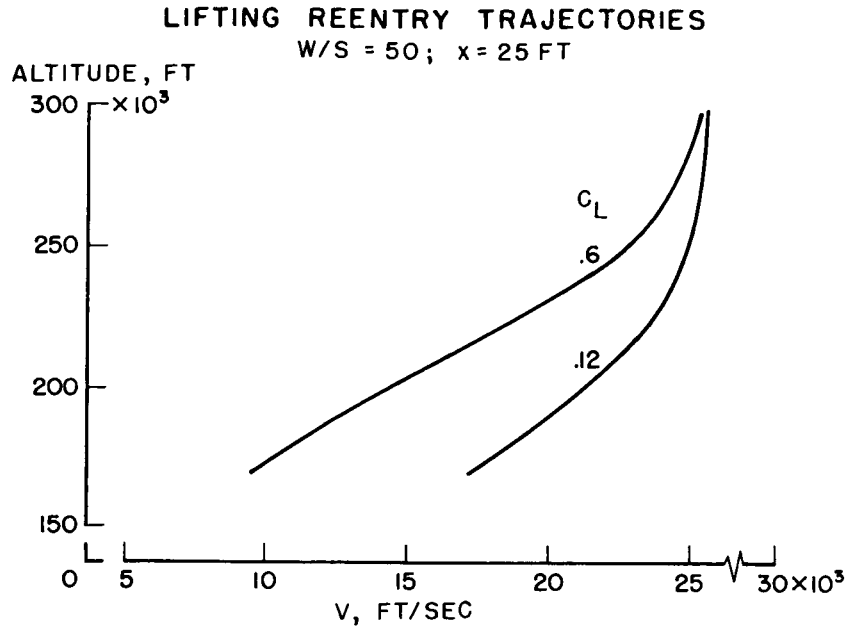

Figure 10

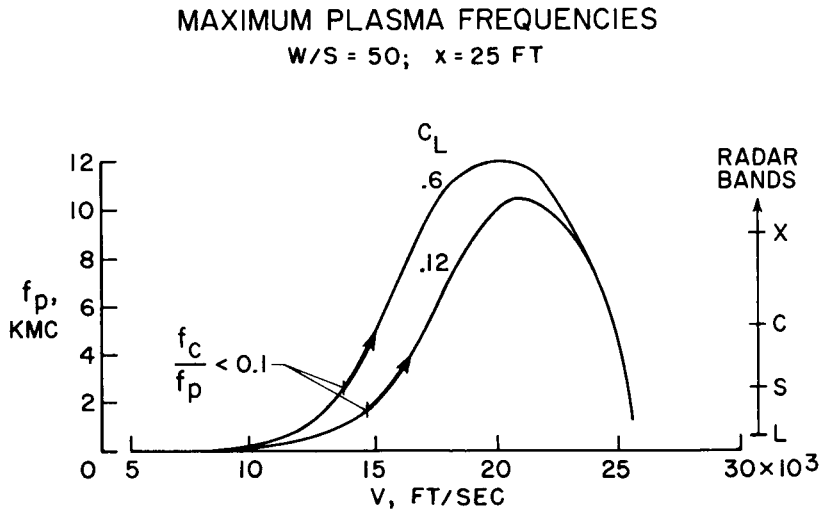

Figure 11

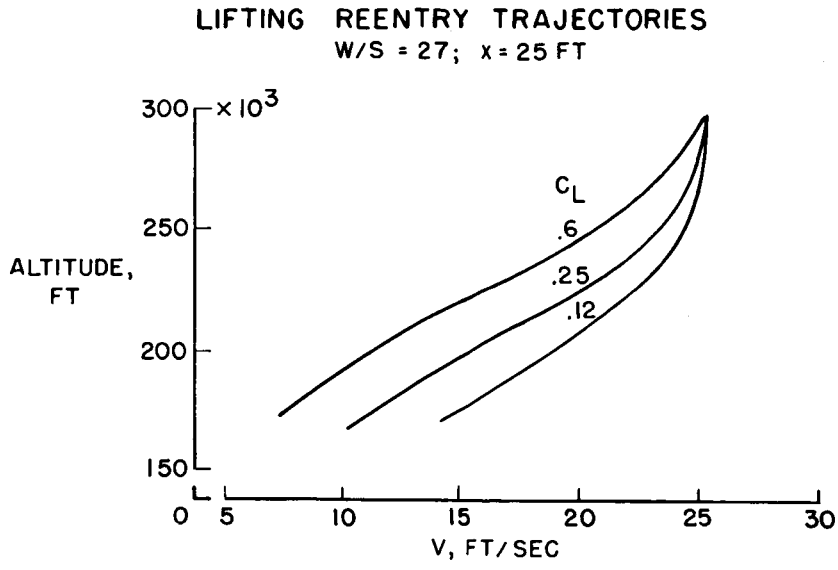

Figure 12

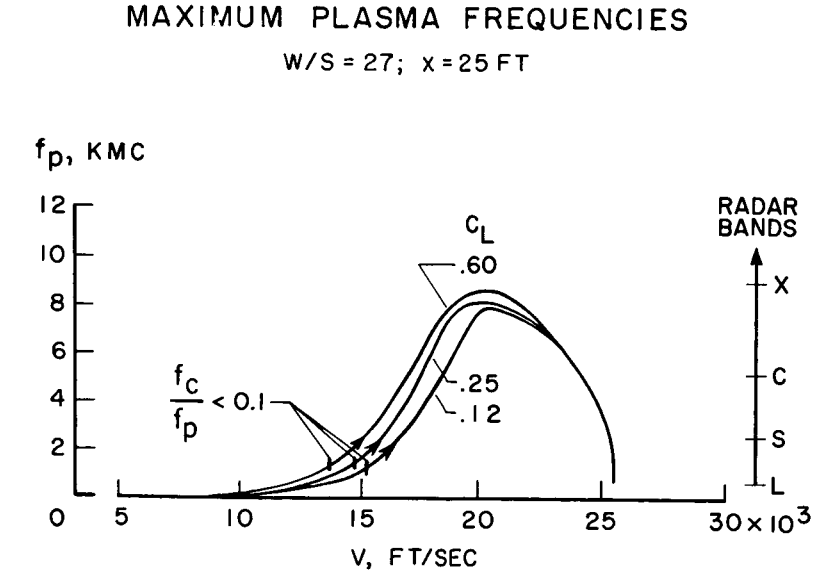

Figure 13

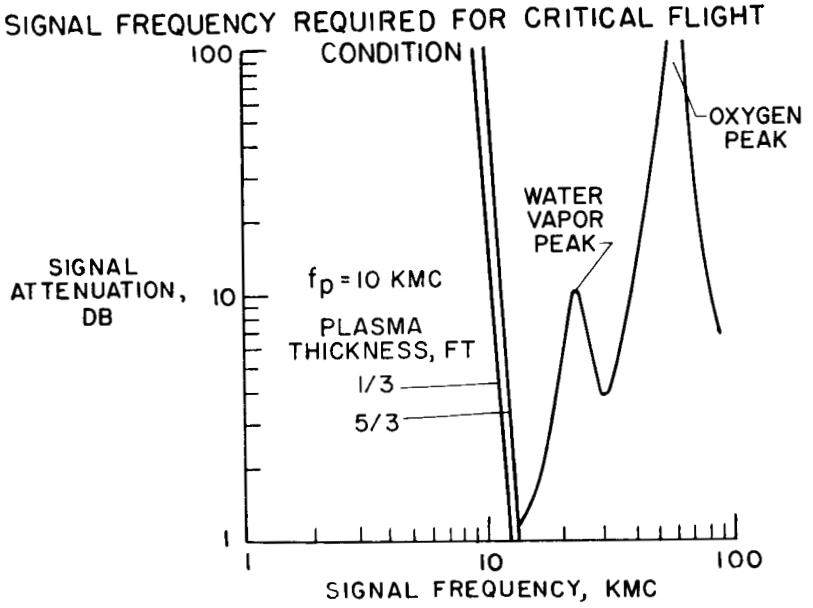
SIGNAL FREQUENCY REQUIRED FOR CRITICAL FLIGHT CONDITION
100
10
1
SIGNAL ATTENUATION, DB
f_p = 10 KMC
PLASMA THICKNESS, FT
1/3
5/3
WATER VAPOR PEAK
OXYGEN PEAK
1
10
100
SIGNAL FREQUENCY, KMC

Figure 14